Proceedings of the American Control Conference
San Diego, California • June 1999

Adaptive Robust Control for Active Suspensions

Supavut Chantranuwathana[1] Huei Peng[2]
Department of Mechanical Engineering and Applied Mechanics
University of Michigan, Ann Arbor, MI 48109-2125
hpeng@umich.edu
Tel: (734) 936-0352, Fax: (734) 647-3170

Abstract

This paper presents a nonlinear active suspension controller, which achieves high performance by compensating for the hydraulic actuator dynamics. The control design problem is decomposed into two loops. At the top is the main loop, which calculates the desired force signal by using a standard LQ design process. An Adaptive Robust Control technique is used to design a force controller such that it is robust against actuator uncertainties. Both State feedback and output feedback algorithms are presented. Simulation results show that the proposed controller works well compared with conventional controllers.

1. Introduction

Automotive suspension systems have been developed over the last 100 years to a very high level of sophistication. Complex kinematic configurations were designed to strike a balance between the complicated functions to be carried out by the suspensions. Most passive suspension systems mainly employ some type of springs in combination with hydraulic or pneumatic shock absorbers. It is commonly accepted that passive suspensions have limited performance because their components can only store or dissipate energy. The idea of adding active components was introduced to improved vehicle handling and ride.

Optimal control techniques have been used intensively in designing active suspension control algorithms ever since the very early days of active suspensions. The Linear Quadratic Gaussian technique, in particular, is popular because trade-offs between multiple objectives (ride quality, handling, packaging, etc.) can be taken care of naturally. Despite a long list of research papers published in this area (see Hrovat 1997), a closer examination shows that many of these algorithms assume that the suspension force can be controlled accurately. Actuators that can push/pull those 2500-pound vehicles at frequencies up to several Hz, however, are extremely expensive. When a less-capable actuator is used, a sub-loop (force control loop) control design needs to be carried out. In actual implementations, an electronically controlled hydraulic actuator is commonly chosen due to its high power to weight ratio. Hydraulic actuators, however, interact with the vehicle dynamics and thus good force tracking is difficult to achieve, especially at high frequencies. As a result, despite of the abundance of simulation results published in the literature, a few experimental verifications have been reported and they are all confined to low disturbance and low frequency regions.

Engelman and Rizzoni (1993) reported that their LQG controller fails to achieve the desired performance since the actuator force had to be kept small to prevent instability. In a recent study conducted at the University of Michigan (Strathearn 1996), LQG controllers were implemented on a quarter-car test rig and they were found to be stable in experiments only at low control gains which give minor performance improvement. It should be noted that in both of these studies, linearized actuator dynamics were used and the LQG controllers were designed based on the augmented plant. It seems fair to say that the control of active suspensions with hydraulic actuators is not trivial, especially for frequencies higher than a few hertz. We believe the difficulty mainly arises from two sources: small stability margins of LQG designs and the interaction between actuator and vehicle dynamics.

The stability of LQG controllers for quarter car models with ideal actuators was studied by Ulsoy et al. (1994). This study shows that LQG controllers have small stability margins, especially when suspension stroke is the sole measured signal. The loop transfer recovery technique was suggested to improve the margin. However, performance will be sacrificed (Birdwell 1990). An alternative solution is to confront the actuator dynamics directly by focusing on the force control loop design. The later approach is taken in our study.

In this paper, we will report the design and simulation results of a nonlinear active suspension controller which achieves high performance by compensating for the hydraulic actuator dynamics. The control design problem is decomposed into two loops. In the main loop, the desired force signal is calculated from a standard LQ design process. In the sub-loop, we will apply the Adaptive Robust Control (ARC) technique to design a force control law. Since LQ designs for active suspensions have been amply reported in the literature, this paper will focus on the design of the sub-loop. In general, a force sensor is necessary for implementing the force control sub-loop. However, due to the fact that good force sensors are usually expensive, another goal of this paper is to design a sub-loop without using force sensors. An asymptotic force observer similar to that proposed by Hedrick (1994) is used where a force sensor is replaced by two accelerometers. Finally, the ARC technique suggested by Yao and Tomizuka (1997) was modified to guarantee force tracking performance when a force observer is used.

The remainder of this paper is organized as follows: The modeling of the quarter-car suspension system studied in this paper is presented in Section 2. The

[1] Graduate Student [2] Assistant Professor

0-7803-4990-6/99 $10.00 © 1999 AACC

control designs are shown in Section 3. The proposed ARC control algorithm is compared against several standard active suspension design techniques in a simulation study in Section 4. Finally, Conclusions are drawn in Section 5.

2. Modeling

A quarter-car suspension system (Fig. 2.1) is studied in this paper. In Fig. 2.1, m_s denotes the vehicle sprung mass, m_{us} is the unsprung mass, k_s is the suspension stiffness, k_{us} is the tire stiffness, c_s is the suspension damping, and c_{us} is the tire damping. x_c, x_w and x_r are the displacement of the vehicle, wheel and road, respectively. An actuator is assumed to present which can exert a force Fa in between m_s and m_{us}.

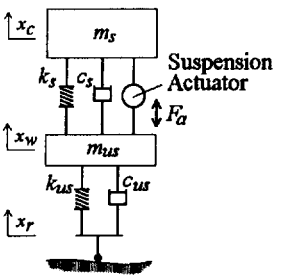

Fig. 2.1 Quarter-Car Model

The linear dynamic equations for this quarter-car suspension are:

$$m_s \cdot \ddot{x}_c = k_s(x_w - x_c) + c_s(\dot{x}_w - \dot{x}_c) + F_a \qquad (2.1)$$

$$m_{us} \cdot \ddot{x}_w = k_{us}(x_r - x_w) + c_{us}(\dot{x}_r - \dot{x}_w) - k_s(x_w - x_c) - c_s(\dot{x}_w - \dot{x}_c) - F_a. \qquad (2.2)$$

which can be written in a state-space form as:

$$\dot{X} = A_1 X + B_1 u \qquad (2.3)$$

where $X = [x_r - x_w, \dot{x}_w, x_w - x_c, \dot{x}_c]^T$ and $u = [F_a, \dot{x}_r]^T$.

The hydraulic actuator is assumed to consist of a spool valve (servo-valve) and a hydraulic cylinder, and is shown in Fig. 2.2. Ps and Pr are the pressure of the hydraulic fluid entering and leaving the spool valve respectively. x_{sp} is the spool valve position. Pu and Pl are the oil pressure in the upper and lower cylinder chambers. $x_w - x_c$ is the hydraulic piston displacement. As the spool valve moves upward (positive x_{sp}), the cylinder upper chamber is connected to the supply line and its pressure increases. In the meantime, the lower chamber is connected to the return line and its pressure reduces. Due to this pressure difference, the hydraulic cylinder will extend (McCloy 1973).

The spool valve displacement (x_{sp}) is assumed to relate to the servo-valve current (i_{sv}) through the following linear transfer function:

$$\frac{Xsp(s)}{Isv(s)} = \frac{Ksv}{\tau s + 1}. \qquad (2.4)$$

However, this dynamics are assumed to be sufficiently fast and will not be used in controller design process. By assuming that (i) the valve opening area is linearly related to the spool valve displacement, (ii) the upstream area is much larger than the orifice area, (iii) the fluid is incompressible, (iv) the piston inertia is negligible, and (v) changes in magnitude of pressures in the two chambers are approximately equal, i.e. $\Delta Pu \approx -\Delta Pl \approx \Delta P$, the force dynamics are

$$\dot{F}_a = \frac{\sqrt{2}Ap \cdot \beta \cdot Kxd}{V} x_{sp} \cdot Sign\sqrt{Ps - sign(x_{sp})F_a / Ap} + \frac{2 \cdot Ap^2 \cdot \beta \cdot Kas}{V} \cdot (\dot{x}_w - \dot{x}_c), \qquad (2.5)$$

where Ap is the average piston area, V is the average volume of each chamber at equilibrium, β is the fluid bulk modulus, Kxd is the orifice flow coefficient, and Kas is the average ratio between suspension stroke and actual actuator cylinder displacement.

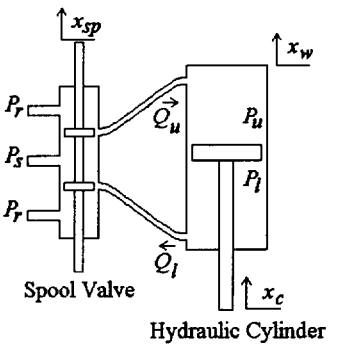

Fig. 2.2 The Electro-Hydraulic Actuator

In summary, Eqs.(2.3) and (2.5) will be used for the controller designs. In simulations, however, a more complicated model will be used. In the simulation model, a more complex version of Eq.(2.5) will be used, which includes cylinder pressures as states. Furthermore, the spool valve dynamics (Eq.(2.4)) will also be included.

3. Controller Design

The objective of the force control loop is to manipulate the spool-valve motion so that the actual force closely tracks the desired force requested by the main loop. The input/output (i_{sv} and Fa) relationship of this control problem is shown in Fig.3.1.

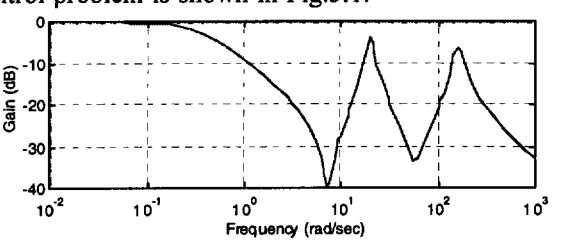

Fig 3.1 Transfer function from servo-valve current to actuator force.

Notice the dips in the magnitude plot at around 1 and 10 Hz are caused by zeros of the transfer function. Traditional design methods such as PID cannot reduce the dips in the closed loop transfer function significantly unless excessively high gains are used. Since the full benefits of active suspensions can be realized only when good tracking up to 5-10 Hz is achieved, more advanced controllers need to be designed. Controllers based on pole-zero cancellation methods can be used only if most of the system parameters are accurately known. However, this is not true for our suspension system. Parameters

such as the hydraulic fluid's bulk modulus can change significantly as the system age. Furthermore, nonlinearity in the hydraulic actuator makes it even more difficult to design good force tracking controllers. This fact was recognized and nonlinear actuator models were included in several recent designs (Alleyne et al. (1993, 1995), Hedrick et al. (1994), Lin et al. (1997)).

Recently, an Adaptive Robust Control (ARC) method was introduced (Yao and Tomizuka 1997) which combines the benefits of Deterministic Robust Control and Adaptive Control techniques. A major advantage of ARC is that both transient and steady-state tracking accuracy can be guaranteed. Furthermore, asymptotic tracking can be achieved when no general uncertainty exists. ARC technique produces a continuous control law as opposed to switching laws commonly deployed in variable structure controllers such as sliding mode controls (Alleyne and Hedrick 1995). Switching controls are undesirable because they excite high frequency resonance of the fluid in the hydraulic system.

3.1 State Feedback ARC

Consider the force dynamics (see Eq. (2.5)):

$$\dot{F}_a = \theta_1[k_1(\dot{x}_w - \dot{x}_c) - k_2 F_a + k_3 u] + d \qquad (3.1)$$

where $k_1 = 2A_p{}^2$, $k_2 = K_p$ and $k_3 = \sqrt{2}A_p K_{xd}$ are known parameters, $\theta_1 = \frac{\beta}{V}$ is an unknown parameter, d denotes general uncertainties arise from unmodeled dynamics and disturbances, and

$$u = x_{sp}\sqrt{P_s - \mathrm{sgn}(x_{sp})F_a / A_p} \qquad (3.2)$$

is the redefined control signal. θ_1 and d are assumed to be bounded and their bounds are known: $0 < \theta_{1m} < \theta < \theta_{1M}$ and $|d| < d_M$. It should be note that an extra term (k_2) was added to make the model more general, as this term is used by several other researchers.

Let F_d to denote the desired force and $e_1 = F_a - F_d$ be the tracking error, a Lyapunov function is chosen to be:

$$V_1 = \frac{1}{2}e_1{}^2 \qquad (3.3)$$

By following a procedure outline in a paper by Yao (Yao 1997), we obtained an ARC control law that consists of two parts: an adaptive part (u_{1a}) and a robust part (u_{1s}). In particular,

$$u = u_{1a} + u_{1s}. \qquad (3.4)$$

The adaptive part is chosen to be

$$u_{1a} = \frac{1}{k_3}\{-k_1(\dot{x}_w - \dot{x}_c) + k_2 F_a + \frac{1}{\hat{\theta}_{1\pi}}(\dot{F}_d + p_1 e_1)\}, \qquad (3.5)$$

where $\hat{\theta}_{1\pi}$ is a bounded projected estimate of θ_1, p_1 is a tunable parameter, and the adaptation law is chosen to be $\dot{\hat{\theta}}_1 = \gamma_1 e_1[k_1\hat{z}_2 - k_2\hat{F}_a + k_3 u_a]$ where $\gamma_1 > 0$. The robust control part is chosen to be:

$$u_{1s} = -e_1\frac{1}{4\theta_{1m}k_3}(\frac{1}{\varepsilon_{11}}\pi_{1M}{}^2(k_1(\dot{x}_w - \dot{x}_c) - k_2 F_a + k_3 u_{1a})^2 + \frac{1}{\varepsilon_{12}}d_M{}^2), \qquad (3.6)$$

where π_{1M} is a positive number such that, $\pi_{1M} \geq |\tilde{\theta}_{1\pi}|, \forall t$, and ε_{11} and ε_{12} are adjustable small positive numbers. Using the control law shown in Eqs.(3.4)-(3.6), it is easy to show that

i) $\dot{V}_1 \leq -p_1 e_1{}^2 + \varepsilon_{11} + \varepsilon_{12}$, (3.7)

ii) when $d \equiv 0$, $\dot{V}_1 \leq -p_1 e_1{}^2 + \tilde{\theta}_{1\pi}\tau_1$ (3.8)

where $\tau_1 = e_1(k_1(\dot{x}_w - \dot{x}_c) - k_2 F_a + k_3 u_{1a}))$. Eq.(3.7) shows that the system is stable and the force tracking error (e_1) is bounded. The transient and final tracking accuracy are adjustable by changing p_1, ε_{11} and ε_{12} and the Lyapunov function is bounded by

$$V(t) \leq V(0)\exp(-2p_1 \cdot t) + \frac{2p_1}{(\varepsilon_{11} + \varepsilon_{12})}(1 - \exp(-p_1 \cdot t)).$$

In addition, Eq. (3.8) implies that the force tracking error converges to zero if the disturbance (d) vanishes. The original control signal x_{sp} can then be found from the Eq. (3.2), i.e.

$$x_{sp}(t) = \frac{u(t)}{\sqrt{P_s - \mathrm{sgn}(u(t))F_a / A_p}}. \qquad (3.9)$$

3.2 Output Feedback ARC

Since force sensors are usually costly and difficult to install, a force observer is implemented. This observer uses three sensors to measure vehicle body acceleration, wheel acceleration and suspension displacement. The main advantage of this observer is that its estimation converges to the true value asymptotically when there is no sensor noise. From Eq.(2.1), we have

$$F_a = m_s\ddot{x}_c - k_s(x_w - x_c) - c_s(\dot{x}_w - \dot{x}_c) \qquad (3.10)$$

Assuming that all the parameters are known and $\ddot{x}_c, x_w - x_c$ are measured, we only need to estimate $\dot{x}_w - \dot{x}_c$ to obtain an estimate of F_a. An intuitive estimation for $\dot{x}_w - \dot{x}_c$ is:

$$\dot{\hat{z}} = A_f\hat{z} + B_f\hat{u} + L(y - C_f\hat{z}) \qquad (3.11)$$

where $\hat{z} = [\hat{z}_1, \hat{z}_2]^T$, $\hat{z}_1 = \hat{x}_w - \hat{x}_c$ and $\hat{z}_2 = \dot{\hat{x}}_w - \dot{\hat{x}}_c$ are the estimated suspension stroke and speed, respectively. $\hat{u}$ is the measured accelerations ($=[\ddot{x}_w, \ddot{x}_c]^T$), y is the measured $x_w - x_c$, L is the observer gain, and $A_f = \begin{bmatrix}0 & 1\\ 0 & 0\end{bmatrix}$, $B_f = \begin{bmatrix}0 & 0\\ 1 & -1\end{bmatrix}$, and $C_f = [1, 0]$. Since A_f, B_f and C_f are constant matrices, they can be used in the observer without uncertainties. Neglecting sensor noises and denoting $\tilde{z}$ as the estimation error (i.e., $\tilde{z} = z - \hat{z}$), we obtain

$$\dot{\tilde{z}} = (A_f - LC_f)\tilde{z}. \qquad (3.12)$$

With this observer, we can proceed to design a controller to drive the estimated force ($\hat{F}_a$) to converge to the desire force (F_d) asymptotically. The asymptotic observer then guarantees that F_a, the actual actuator force, also converges to F_d asymptotically.

Let $A_f - LC_f = \begin{bmatrix} a_3 & a_4 \\ a_1 & a_2 \end{bmatrix}$ and $L = \begin{bmatrix} l_1 \\ l_2 \end{bmatrix}$, the estimated force equation can be written as:

$$\dot{\hat{F}}_a = \theta_1[k_1\hat{z}_2 - k_2\hat{F}_a + k_3 u] + d + c_s a_1 \tilde{z}_1 + (c_s a_2 + c_s\theta_1 k_2 + \theta_1 k_1)\tilde{z}_2 \quad (3.13)$$

Note that Eq. (3.13) has extra terms in comparison to Eq. (3.1). The output feedback ARC controller can be designed in a fashion similar to that of the state feedback ARC except that a nonlinear damping term is added to counteract the destabilizing effect of the observer (Krstic 1995). The Lyapunov function is chosen to be

$$V = \frac{1}{2}e_1^2 + \tilde{z}^T P \tilde{z}. \quad (3.14)$$

where P is the positive definite solution of a Lyapunov equation $P(A_f - LC_f) + (A_f - LC_f)^T P = -Q$. The matrix $Q = \begin{bmatrix} \rho_{11} + \sigma_{11} & 0 \\ 0 & \rho_{12} + \sigma_{12} \end{bmatrix}$, where σ_{11}, σ_{12} are arbitrary positive numbers and ρ_{11}, ρ_{12} are control parameters that can be freely selected. The ARC control law for $u(t)$ consists of three parts: an adaptive part, a robust part, and a damping part. In particular,

$$u = u_{1a} + u_{1s} + u_{1d} \quad (3.15)$$

The adaptive part is chosen as

$$u_{1a} = \frac{1}{k_3}(k_2\hat{F}_a - k_1\hat{z}_2 + \frac{1}{\hat{\theta}_{1\pi}}\dot{F}_d - \frac{p_1}{\hat{\theta}_{1\pi}}e_1) \quad (3.16)$$

where $\hat{\theta}_{1\pi}$ is a bounded projected estimate of θ_1 and p_1 is used for tuning the controller. The adaptation law is chosen to be $\dot{\hat{\theta}}_1 = \gamma_1\tau_1 = \gamma_1 e_1[k_1\hat{z}_2 - k_2\hat{F}_a + k_3 u_a]$, where $\gamma_1 > 0$ is a tunable gain. The robust control part is chosen as:

$$u_{1s} = -\frac{1}{4\theta_{1m}k_3}e_1\{\frac{1}{\varepsilon_{11}}K^2(k_1\hat{z}_2 - k_2\hat{F}_a + k_3 u_{1a})^2 + \frac{1}{\varepsilon_{12}}d_M{}^2\}, \quad (3.17)$$

where ε_{11} and ε_{12} are small positive numbers. Finally, the damping part is chosen as

$$u_{1d} = -\frac{1}{4\theta_{1m}k_3}e_1\{\frac{1}{\rho_{11}}(c_s a_1)^2 + \frac{1}{\rho_{12}}\Phi^2\}, \quad (3.18)$$

where $\rho_{11}, \rho_{12} > 0$, K is the bound of the projected estimation error, and Φ is a bound of the absolute value of the term multiplying $\tilde{z}_2$ in Eq.(3.13).

With the above defined control law, it can be shown that

i) $\dot{V} \le -p_1 e_1^2 + \varepsilon_{11} + \varepsilon_{12} - \sigma_{11}\tilde{z}_1^2 - \sigma_{12}\tilde{z}_2^2$ (3.19)

and

ii) $\dot{V} \le -W + \tilde{\theta}_{1\pi}\tau_1$, when $d \equiv 0$, (3.20)

where $W = p_1(e_1)^2 + \sigma_{11}\tilde{z}_1^2 + \sigma_{12}\tilde{z}_2^2$. Eq. (3.19) implies that the estimated force tracking error ($\hat{F}_a$ - F_d) is bounded and its transient and final tracking accuracy can be adjusted by changing p_1, ε_{11} and ε_{12}. In addition, Eq.(3.20) implies that the estimated force tracking error converges to zero if no disturbance (d) is present.

Since F_a is not measured, x_{sp} cannot be calculated from Eq. (3.9). We choose to use an alternative approach which allows discontinuity in the control law. For example, x_{sp} can be calculated from:

$$x_{sp} = \frac{u}{\sqrt{P_s - \mathrm{sgn}(u)(\hat{F}_a - \mathrm{sgn}(e_1)\psi_M)/A_p}} \quad (3.21)$$

where $\psi_M \ge C_s|\tilde{z}_2|, \forall t$. When Eq. (3.21) is used to calculate x_{sp}, the inequality in Eq (3.19) and (3.20) will be preserved.

4. Simulation Results

Two sets of simulations were carried out to verify the performance of the proposed Active Suspension (AS) controller. In the first set of simulations, we assumed that all the states are available and the actuator force is also measured. In the second set of simulations, only three signals are assumed to be measured: sprung and unsprung mass accelerations, and suspension stroke.

We simulated the following systems: a passive suspension (the worst case), an AS with PID sub-loop, an AS with ARC sub-loop and an LQ AS without sub-loop dynamics (the best case). The main loop controllers for all of the AS cases are designed using standard LQ techniques. The cost function was chosen to be:

$$J = \int_0^\infty \eta(x_r - x_w)^2 + 1/\eta(\ddot{x}_c)^2 + r_2(x_w - x_c)^2 + r_3 Fa^2 dt \quad (4.1)$$

Four sets of weights were used: [r1,r2,r3] = [500,10,3e-10], [400,10,3e-10], [300,10,3e-10] and [200,10,3e-10]. Measurement noise and uncertainty in actuator dynamics were also created. In particular, the fluid bulk modulus was assumed to be 75% lower than its nominal value. Fig. 4.1 shows the cost (integrate Eq.(4.1) for 10 sec) of each design. The values are normalized against the cost of the passive system. It can be seen that the ARC controller performs much better than the PID controller.

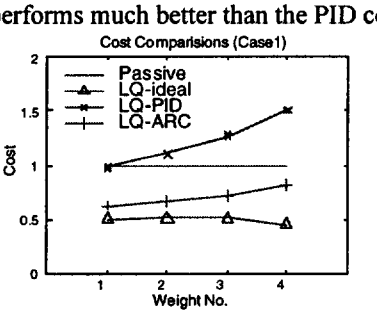

Fig. 4.1 Cost Comparison (Case 1).

In the second (output-feedback) case, only three measurements were used: $x_w - x_c$, $\ddot{x}_c$, and $\ddot{x}_w$. Hence, the main loop controller was replaced with an LQG controller. The force observer described in section 3 was used to provide force estimates for all the AS designs. The ARC controller was replaced by the output feedback ARC controller. Furthermore, a single-loop design (Engelman et al. 1993) which included a linearized actuator dynamic was also designed using LQG techniques. For the state feedback part of this controller, the above cost function was modified to include a very

small weighting on the new control signal (x_{sp}). For the observer part, designing a Kalman filter is straightforward since data on measurement noises and road excitations are known. Fig 4.2 shows the comparisons of cost values (integrate Eq. 4.1 for 10 sec) of each system. It can be seen that the proposed ARC controller performs best (close to the ideal controller).

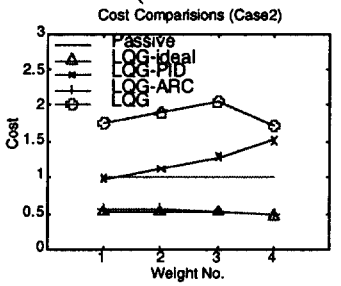

Fig 4.2 Cost Comparison (Case2)

Tables 4.1 and 4.2 show details of the simulation results. A set of data from each case is presented. Except for the cost (J), other entries in this table are the root mean square value of the corresponding signal. It could be seen that the performance gain by the ARC controller partially results from its higher controller signal. The LQG have higher control signal than that of the LQG-PID controller but performs much worst. It can also be seen that the LQG-ARC controller performs better than the LQ-ARC controller. This is due to the higher control signal used by the LQG-ARC controller resulted from the extra damping term.

Table 4.1 Detail of Simulation Results for Case 1

		Passive	LQ-ideal	LQ-PID	LQ-ARC
No. 1	$x_r - x_w$	2.4e-3	1.7e-3	2.3e-03	2.1e-3
	$\ddot{x}_c$	0.67	0.6	1.0	0.56
	J	4.9e-2	2.5e-2	4.8e-2	3.1e-2
	x_{sp}	N/A	N/A	3.7e-05	5.2e-5

Table 4.2 Detail Simulation Results for Case 2

		Passive	LQ-ideal	LQ-PID	LQ-ARC	LQG
No. 1	$x_r - x_w$	2.4e-3	1.7e-3	2.3e-3	1.8e-3	3.7e-3
	$\ddot{x}_c$	0.67	0.6	1.0	0.63	0.63
	J	4.9e-2	2.5e-2	4.8e-2	2.7e-2	8.6e-2
	x_{sp}	N/A	N/A	5.2e-5	3.6e-4	1.0e-4

It should be noted that these controllers may perform well in simulations if their gains are high enough. However, it is clear that high gain controllers may cause instability in actual applications. To ensure that each controller has some degree of stability margin, extra poles were added at high frequency (100Hz) and the gain of each controllers (for the PID and ARC controllers) were maintained so that the system is stable. In addition, a 10 Hz pre-filter was also used to supply $\dot{F}_d$ which is required by the ARC controllers.

5. Conclusions and Future Works

In this paper, we designed a controller for force control loop. One of the main benefits of this approach is that, if a good force control loop is obtained, it is likely that many of the existing AS controllers can be implemented with improved performance. A modified ARC technique was proposed to maintain stability when force sensor is removed form the system. Simulation results show that the proposed ARC controllers work very well compare to a PID controller. These comparisons are between controllers with the same two-loop approach. A linear LQG controller that is a single-loop design was also introduced for comparison. However, this controller performs poorly.

Future works include experimental verifications and extra simulations. Simulations using other weights are necessary to provide a better overview of the performance improvement.

Acknowledgement

The authors wish to thank Dr. D. Hrovat of the Ford Motor Company for his generous support of this study.

References

Alleyne, A., Hedrick, J.K., (1995) "Nonlinear Adaptive Control of Active Suspension," *IEEE Trans. on Cont. Sys. Tech.*, v3, n1, pp94-101

Alleyne, A., Neuhaus, P.D., Hedrick, J.K., (1993) "Application of Nonlinear Control Theory to Electronically Controlled Suspensions," *Vehicle System Dynamics*, Vol. 22, pp.309-320

Birdwell, J.D. (1989) "Evolution of a Design Methodology for LQG/LTR," *IEEE Control System Magazine*, vol.9, n3, pp.73-78

Engelman, G. H., Rizzoni, G., (1993) "Including the Force Generation Process in Active Suspension Control Formulation," Proc. of the 1993 American Control Conference, pp.701-705

Hedrick, J.K., Rajamani, R., Yi, K., (1994) "Observer Design for Electronic Suspension Applications," *Vehicle System Dynamics*, Vol.23, pp.413-440

Hrovat, D., (1997) "Survey of Advanced Suspension Developments and Related Optimal Control Applications," *Automatica*, v 33 n 10, pp.1781-1817.

Krstic, M., Kanellakopoulos, I., Kokotovic, P., (1995) *Nonlinear and Adaptive Control Design*, John Wiley & Sons.

Lin, J., Kanellakopoulos, I., (1997) "Nonlinear Design of Active Suspension," *IEEE Control System Magazine*, pp.45-59.

McCloy, D., (1973) *The Control of Fluid Power*, Wiley.

Rajamani, R., Hedrick, J.K., (1995) "Adaptive Observers for Active Automotive Suspensions: Theory and Experiment," *IEEE Trans. on Control Systems Technology*, v3, n1, pp.86-93.

Strathearn, R.R., (1996) *Active Suspension Design and Evaluation Using a Quarter Car Test Rig*, Master's Thesis, University of Michigan.

Ulsoy, A.G., Hrovat, D., Tseng, T. (1994) "Stability Robustness of LQ and LQG Active Suspension," *ASME Journal of Dynamic Systems, Measurement, and Control*, v116, pp.123-131.

Yao, B., Tomizuka, M., (1997), "Adaptive Robust Control of SISO Nonlinear Systems in a Semi-strict Feedback Form," Automatica, v.33, n5, pp. 893-900.